Desalination and Water Treatment
www.deswater.com
doi: 10.1080/19443994.2014.998292

57 (2016) 5004–5012
March

Taylor & Francis
Taylor & Francis Group

Adsorption of Hg(II) from aqueous solution using amino-functionalized graphite nanosheets decorated with Fe_3O_4 nanoparticles

Yingxia Ma*, Peiqing La, Wenjuan Lei, Cuiping Lu, Xueyan Du

State Key Laboratory of Advanced Processing and Recycling of Nonferrous Metals, School of Materials Science & Engineering, Lanzhou University of Technology, Lanzhou 730050, P.R. China, Fax: +86 931 2976702; emails: mayx2011818@163.com (Y. Ma), pqla@lut.cn (P. La), catherinelwj@163.com (W. Lei), woshilcp@163.com (C. Lu), duxy@lut.cn (X. Du)

Received 20 January 2014; Accepted 4 December 2014

ABSTRACT

In this study, the property of 3-aminopropyltriethoxysilane modified graphite nanosheets (GNS) decorated with Fe_3O_4 nanoparticles (Fe_3O_4-GNS-NH_2 hybrids) for adsorption of Hg (II) in aqueous solution were evaluated by batch methods. The adsorption mechanism was also studied by X-ray photoelectron spectroscopy. The effect of factors, such as pH, contact time, initial concentration of Hg(II) and the GNS content (wt.%) for Fe_3O_4 in Fe_3O_4-GNS-NH_2 hybrid materials on Hg(II) removal were investigated. The equilibrium data were analyzed using the Langmuir and Freundlich isotherm models. The pseudo-first-order adsorption and the pseudo-second-order adsorption models were used to fit kinetics experimental data. The results showed that the main adsorption mechanism for Hg(II) was the formation of N-metal ions chemical complex, the solution pH value had a major impact on Hg(II) adsorption with optimal removal observed around pH 4.0–6.0, the Langmuir isotherm model was found to be suitable for the Hg(II) adsorption and the adsorption kinetic followed the pseudo-second-order equation for Fe_3O_4-GNS-NH_2 hybrid materials.

Keywords: 3-aminopropyltriethoxysilane; Hybrid materials; Hg(II); Adsorption; Mechanism

---

1. Introduction

Concerning health and environmental problems, water pollution represents major challenges facing the global society [1]. Mercury is one of the most toxic contaminants affecting the environment. It gradually bioaccumulates in the aquatic environment and finally reaches the human being through food chains (mainly fish) causing various neurological disease and disorders [2]. Therefore, removal of mercury in water and wastewater is important. Among several methods for the removal of heavy metals from solutions such as membrane separation, filtration, chemical oxidation or reduction, evaporative recovery, ion exchange and reverse osmosis, lime precipitation, electroplating [3–10], adsorption technique proves to be one of the most efficient methods of cleaning the environment of heavy metal pollutant. Magnetic loaded adsorbent materials with high separation efficiency, simple manipulation process, kind operation conditions and easy specifically functional modifications have recently received increasing attention for heavy metal removal from aqueous media [11–19].

Graphene, a single two-dimensional layer of carbon atoms bonded together in the hexagonal graphite lattice, is a rising star in the material science and

---

*Corresponding author.

technology because of its excellent characters including high values of Young's modulus, fracture strength, thermal conductivity, specific surface area and fascinating transport phenomena, etc. [20]. These combinations of extraordinary physical properties provide such new materials a wide range of potential applications in many technological fields [21]. In recent years, graphene-based materials have been studied as the absorbents for removal of heavy metal ions from aqueous solution [22,23]. Fang et al. [24] demonstrated the use of amination graphene oxide (GO-NH_2) nanosheets for Co (II) ions removal. However, the extensive use of graphene-based materials has been heavily hindered by their exorbitant price. In our previous studies [25], graphite nanosheets (GNS i.e. multilayer graphene oxide) with a promising low cost alternative to others graphene-based materials were prepared. As we all known, Fe_3O_4 nanoparticles have been widely utilized in biological and environmental applications due to they have low toxicity, high bio-compatibility and considerably high saturation magnetization. On account of multifunctional hybrid materials that take advantages of both the unique properties of graphene and the functional materials, Fe_3O_4-GNS hybrid materials were synthesized by an inverse coprecipitation method [25]. Considering that the Fe_3O_4-GNS hybrid materials had a flexible interleaved structure, a large specific surface area, good thermal stability, high magnetic sensitivity and allow the rapid separation of target molecules from the medium by applying an appropriate magnetic field, the amino functionalization of the materials with 3-aminopropyltriethoxysilane (APTES) were used as adsorbents for the removal of Hg(II) from aqueous solution in this work.

2. Experiment

2.1. Materials

Natural flake graphite (NFG) 50 BS mesh, with the purity of 99 wt% was supplied by ShanDong Qingdao Tianhe Graphite Company (China). All the other materials were obtained from Tianjin Guangfu Fine Chemical Research Institute (China), used as received without any further purification.

2.2. Characterization

The X-ray photoelectron spectroscopy (XPS) analysis was carried out on an ESCALAB210 instrument at a pressure greater than 10^{-6} Pa. The general scan C1s, O1s, N1s, Fe2p and Hg4f core level spectra were recorded with unmonochromatized Mg Kα radiation (photon energy: 1,253.6 eV). A thermostat oscillator (Hai Sheng Da HQD 150 L) was used for shaking all of the solutions. The concentrations of Hg(II) in aqueous solution were determined using a PERSEE TU-1810 UV–vis spectrophotometer by monitoring the absorbance at 610 nm. The pH of solutions was determined using a HANNA pH meter.

2.3. Adsorbents preparation

Fe_3O_4-GNS-NH_2 were synthesized according to our previous work [25]. Firstly, NFG was treated by oxide intercalation, thermal expansion and sonication exfoliation to produce GNS. Secondly, GNS decorated with Fe_3O_4 nanoparticles were synthesized by an inverse coprecipitation method with a given amount of GNS, 40 mL of 0.5 M NaOH aqueous solutions, 60 mL of ethanol aqueous solution (1/1, v/v) containing 0.002 mol $FeSO_4·7H_2O$ and 0.004 mol $FeCl_3·6H_2O$ to obtain Fe_3O_4-GNS. Lastly, Fe_3O_4-GNS were modified with APTES. The obtained products were denoted as Fe_3O_4-GNS-NH_2.

2.4. Adsorption experiments

Hg(II) adsorption on Fe_3O_4-GNS-NH_2 hybrids were performed in batch experiments. The experimental Hg(II) aqueous solutions (5–300 mg/L) were prepared by diluting the stock solution of Hg(II) (1,000 mg/L) that was prepared by dissolving an accurately weighed amount of mercuric chloride ($HgCl_2$) in distilled water. For batch tests, a given amount of Fe_3O_4-GNS-NH_2 hybrids (0.1 g) were added into $HgCl_2$ aqueous solution (50 mL) at a known concentration, constant temperature of 30˚C and constant rate 150 rpm in a thermostat oscillator under dark environment. After a desired period of adsorption, the Fe_3O_4-GNS-NH_2 hybrids adsorbed Hg(II) were removed out applying a magnetic field and the Hg(II) content in the residual solution was measured by UV–vis using rhodamine 6G [26]. The sorption capacity of Hg(II) onto the Fe_3O_4-GNS-NH_2 hybrids was calculated according to the equation as given below:

$$Q = (C_0 - C)\frac{V}{W} \tag{1}$$

where Q is the sorption capacity of Hg(II) on Fe_3O_4-GNS-NH_2 hybrids (mg g^{-1}), C_0 and C is the initial and outlet concentration of Hg(II) in solution (mg L^{-1}), respectively, V is the volume of the Hg(II) solution (L) and W is the mass of the Fe_3O_4-GNS-NH_2 hybrids (g) used.

The initial pH value of Hg(II)-containing aqueous solution was carefully adjusted between 2 and 7 with 0.1 M HCl or 0.1 M NaOH before the adsorption experiments and not controlled during the adsorption process. Two linearized adsorption models of Frundlich and Langmiur isotherms were applied to analyze adsorption equilibrium. The adsorption kinetics of Fe_3O_4-GNS-NH_2 hybrids for Hg(II) were studied by using the pseudo-first-order and pseudo-second-order kinetic equations.

3. Result and discussion

3.1. Adsorption mechanism

XPS spectra of both survey and high-resolution scans for the key elements on Fe_3O_4-GNS-NH_2 hybrids before and after Hg(II) adsorption (Fig. 1) were investigated to gain adsorption mechanism.

In Fig. 1(a), the element contents (C 1s, N 1s, O 1s and Fe 2p) on Fe_3O_4-GNS-NH_2 hybrids were demonstrated by XPS surface analysis. From Fig. 1(b), it can be clearly seen that a new peak for Hg 4f became visible for Fe_3O_4-GNS-NH_2 hybrids after Hg(II) adsorption, suggesting the successful adsorption of mercury on the surface of Fe_3O_4-GNS-NH_2 hybrids. Fig. 1(c) shows that the colour of the Hg(II)-containing rhodamine 6G aqueous solutions (Fig. 1(cB)) before Fe_3O_4-GNS-NH_2 hybrids adsorption was distinct difference from the rhodamine 6G aqueous solutions (Fig. 1(cR)). After Fe_3O_4-GNS-NH_2 hybrids adsorption, the colour of the Hg(II)-containing rhodamine 6G aqueous solutions (Fig. 1(dA)) was very close to the rhodamine 6G aqueous solutions (Fig. 1(dR)), which further indicated that the Fe_3O_4-GNS-NH_2 hybrids for Hg(II) removal was very effective.

Fig. 1(e) shows the high resolution XPS Hg4f spectra of the Fe_3O_4-GNS-NH_2 hybrids after Hg(II) adsorption. A pair of doublet-peaks appeared, which could be assigned to Hg4f 5/2 and Hg4f 7/2 with binding energies at 104.8 and 100.8 eV, respectively. These peaks were decomposed into only one component which could be assigned to be adsorbed Hg_2Cl_2 [11]. Previous literature [27] reported that the binding energy of Hg4f 7/2 of the most appropriate reference compounds are as follows: 101.4 eV ($HgCl_2$), 108.0 eV (HgO) and 99.8 eV (Hg metal). For Fe_3O_4-GNS-NH_2 hybrids, it is possible to assume that the adsorbed mercury species is only in Hg_2Cl_2 form. This might be because Hg(II) had been completely reduced to Hg(I) which combined free chloride ions in solution to form Hg_2Cl_2. The reduction reaction might happen via electron transport. Furthermore, after the adsorption of Hg(II), the binding energy of N1sa was increased from 401.42 to 405.77 eV (Table 1). This shift can also be attributed to the protonation of nitrogen sites which were submitted to a charge transfer from amino sites to mercury. It might be due to the formation of N-metal ions [28]. From the XPS analysis, it could be

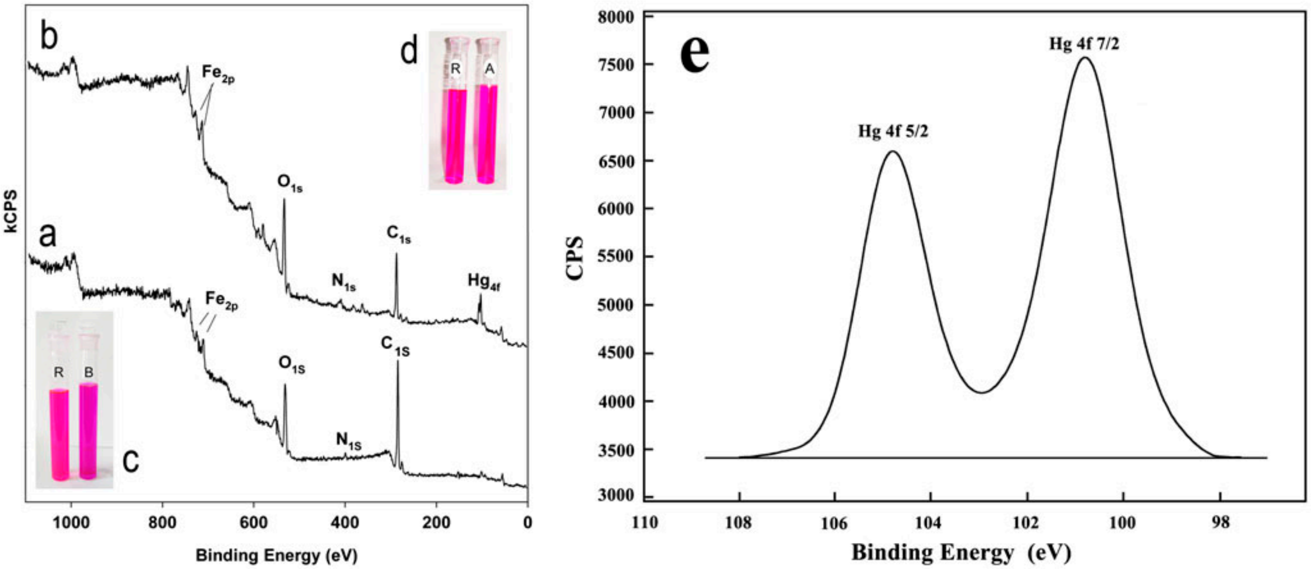

Fig. 1. The survey XPS spectra of Fe_3O_4-GNS-NH_2 hybrids before (a) and after (b) Hg(II) adsorption, the Digital photo of rhodamine 6G aqueous solutions (cR, dR) and Hg(II)-containing rhodamine 6G aqueous solutions using Fe_3O_4-GNS-NH_2 hybrids before (cB) and after (dA) adsorption, the Hg4f XPS spectra of Fe_3O_4-GNS-NH_2 hybrids after Hg(II) adsorption (e).

Table 1
Distribution of elements species on Fe_3O_4-GNS-NH_2 before and after Hg(II) adsorption

Element	Peak BE (eV)	Fe_3O_4-GNS-NH_2 (at%)	Fe_3O_4-GNS-NH_2-Hg (at%)
Hg4f	100.78	–	1.979
C1s	285.00	29.21	25.49
O1s	531.32	26.28	35.52
Fe2p	710.79	4.69	10.89
N1s	399.7	1.45	0.36
N1sa	401.42	0.91	–
N1sa	405.77	–	1.145

concluded that the amine groups was involved in Hg (II) adsorption. The main adsorption mechanism for Hg(II) was complexation.

Meanwhile it can be seen from Table 1 after Hg(II) adsorption, O1s content increased from 26.28 to 35.52 atom% and Fe2p content also increased from 4.69 to 10.89 atom%. These results are mainly due to the dissipation of APTES which was entrapped not bonded on Fe_3O_4-GNS hybrids in the process of adsorption.

3.2. *Adsorption of Hg(II)*

3.2.1. *The contribution of GNS in the Fe_3O_4-GNS-NH_2 hybrids for Hg(II) adsorption*

In order to investigate the adsorption capacity contribution of GNS, the different mass ratios (GNS to Fe_3O_4) were prepared and used to adsorb Hg(II), respectively. Fig. 2 shows the adsorption results, with the increase of the GNS in the hybrids, the adsorbed Hg(II) amount per unit mass of the hybrids increases firstly and then decreases. This phenomenon can be explained by further understanding the characters of Fe_3O_4-GNS-NH_2 hybrids used in the study. According to our previous report [25], GNS possess an open porous system and a flexible interleaved structure which play a "flexible confinement" function to enwrap Fe_3O_4 particles and prevent the agglomeration of pulverized Fe_3O_4. Meanwhile, Fe_3O_4 particles separate GNS and prevent their restacking. With the increase of the GNS, the pore structure and surface area increase in the Fe_3O_4-GNS-NH_2 hybrids which could provide large numbers of adsorption sites for Hg(II). When GNS content is excessive, the dispersity of GNS decreases in the hybrids which reducing the accessible surface area and resulting in the sorption capacity decreases.

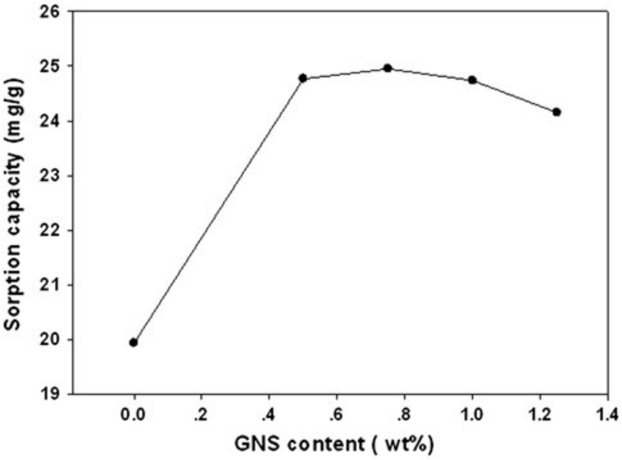

Fig. 2. Effect of the different GNS content (wt%) for Fe_3O_4 in Fe_3O_4-GNS-NH_2 hybrids on the adsorption Hg(II) amount of the hybrids from aqueous solutions (C_0: 50 mg/L, 30℃, and pH 6).

3.2.2. *Effect of pH*

The effect of solution pH on the adsorption Hg(II) of Fe_3O_4-GNS-NH_2 hybrids from aqueous solutions was investigated in the pH ranges of 2.0–7.0 at 30℃ for 24 h as shown in Fig. 3.

The extractability of the cations from the solution phase is pH dependent because of its effect on the solubility of the metal ions, concentration of the counter ions on the functional groups of the adsorbent and the degree of ionization of the adsorbate during reaction [29]. It can be observed from the results that the adsorption capacity of Hg(II) increased enormously with increasing the pH value from 2.0 to 4.0, and reached a plateau value with pH range from 4.0 to 6.0, and then decreased at pH 7.0. A similar phenomenon was observed by Ma et al. [30]. Adsorption capacity may be affected both by species of Hg(II) and the accessibility to the binding sites. As reported [31,32], in the presence of Cl^-, the dominant Hg(II) species is Hg $(OH)^+$ and $Hg(OH)_2$ at $pH > 4.0$ and $HgCl_2$ at $pH < 3.0$. Compared with Hg^{2+}(aq) species of relatively larger hydrated sizes, $Hg(OH)^+$ and $Hg(OH)_2$ species has

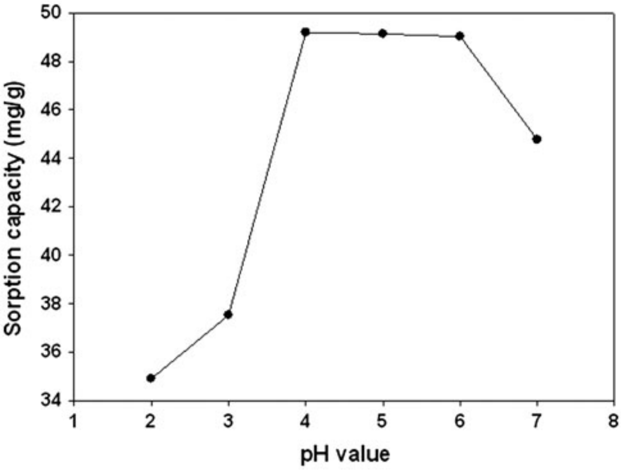

Fig. 3. Effect of solution pH on the adsorption Hg(II) of Fe_3O_4-GNS-NH_2 hybrids from aqueous solutions (contact time: 24 h, 30℃, C_0: 100 mg/L).

higher affinity to nitrogen-containing binding sites [11,33]. Therefore, the adsorption capacity stayed high at pH 4.0–6.0.

Additionally, above results could also be explained by zeta potential indicated in Fig. 4. It was obvious that zeta potentials of the Fe_3O_4-GNS-NH_2 hybrids decreased with increasing pH, which indicated that the surface of Fe_3O_4-GNS-NH_2 hybrids is positively charged in the pH ranges. At low pH, large number of H^+ protonated the amino groups on the surface of Fe_3O_4-GNS, the transformation of NH_2 into NH_3^+ made the electrostatic attraction between Fe_3O_4-GNS-NH_2 hybrids and heavy metal ions was relatively weak. With the pH increasing, the number of positive charges on Fe_3O_4-GNS-NH_2 hybrids decreased and the repulsion between heavy metal ions and positive charge on Fe_3O_4-GNS-NH_2 hybrids weakened, the chelating ability of amino groups toward heavy metal ions strengthened, which contributes to the increase of the adsorption capacity of Fe_3O_4-GNS-NH_2 hybrids for heavy metal ions. Further increasing the pH 7.0 decreased the adsorption, possibly due to the fact that $Hg(OH)_2$ species formed at pH 7.0 have a higher formation constant and can steadily stay in the equilibrium solutions.

3.2.3. Effect of contact time

The effect of contact time on the adsorption Hg(II) amount of Fe_3O_4-GNS-NH_2 hybrids from aqueous solutions was investigated. The adsorption data for Hg(II) uptake vs. contact time for a fixed adsorbent amount are shown in Fig. 5. It was observed that the initial rate was very rapid within the first few hours and slowed down gradually with approaching equilibrium. The results show that the adsorption Hg (II) amount of Fe_3O_4-GNS-NH_2 hybrids tends to equilibrium with 12 h of contact time.

3.2.4. Effect of initial Hg(II) concentration

The effect of the initial Hg(II) concentration on the adsorption Hg(II) amount of Fe_3O_4-GNS-NH_2 is shown in Fig. 6. The results showed that with the increase of initial concentration, the adsorption capacity at equilibrium time was promoted by the increased drive force which attributing to the concentration

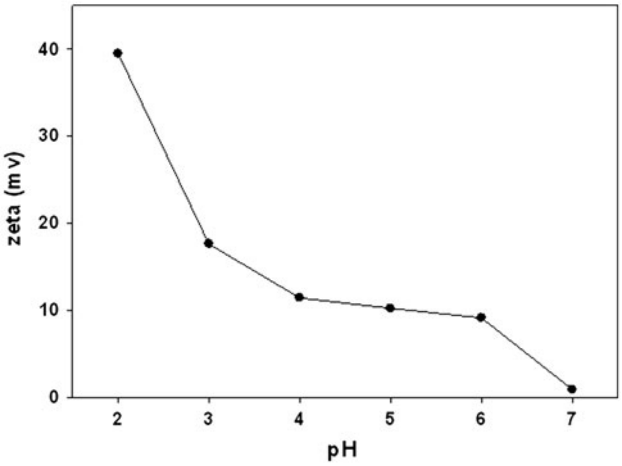

Fig. 4. Effect of aqueous solution pH on Zeta potentials of Fe_3O_4-GNS-NH_2 hybrids.

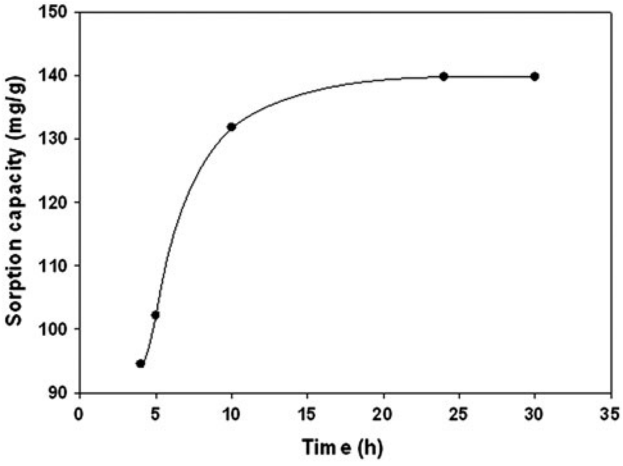

Fig. 5. Effect of contact time on the adsorption Hg(II) amount of Fe_3O_4-GNS-NH_2 hybrids from aqueous solutions (30℃, pH 6 and C_0: 200 mg/L).

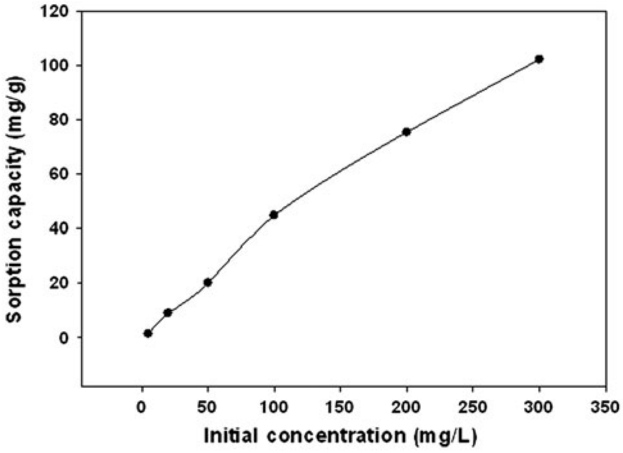

Fig. 6. Effect of initial Hg(II) concentration on the adsorption Hg(II) amount of Fe_3O_4-GNS-NH_2 hybrids from aqueous solutions (30℃, pH 6).

variance of Hg(II) between solution and the hybrids. The experimental results demonstrate that the initial Hg(II) concentration plays an important role in the adsorption of Hg(II).

3.2.5. Adsorption isotherm of Hg(II)

The adsorption equilibrium is usually described by an isotherm equation which expresses the relationship between metal ions adsorbed onto the adsorbent and metal ions in the solution and further demonstrates the surface properties and affinity of the adsorbent. Both the Langmuir and the Freundlich equations were used to describe and analyze the sorption isotherm of Hg(II) by Fe_3O_4-GNS-NH_2 hybrids, which are expressed as follows [34,35]:

$$\frac{C_e}{Q_e} = \frac{1}{K_L Q_{max}} + \frac{C_e}{Q_{max}} \quad (2)$$

$$\text{In} Q_e = \text{In} K_F + \frac{1}{n} \text{In} C_e \quad (3)$$

where Q_e and Q_{max} are the equilibrium adsorption capacity ($mg\,g^{-1}$) and maximum adsorption capacity ($mg\,g^{-1}$), respectively, C_e is the concentration of Hg(II) at equilibrium time ($mg\,L^{-1}$), K_L is Langmuir constant ($L\,mg^{-1}$), K_F ($mg\,g^{-1}$) and n are Freundlich constants.

The calculated correlation coefficients (R) and parameters of Langmuir and Freundlich model were listed in Table 2. As seen from Table 2, the Langmuir model gave the higher R values (0.9992) than Freundlich model (0.8573) at the studied temperature, showing that the Langmuir model describe the experiment data more precisely than the Freundlich model. According to the literature [36], the basic assumption of the Langmuir theory is that uptake of metal ions occurs on a homogenous surface by monolayer adsorption without any interaction between adsorbed ions that is all the adsorption sites have equal adsorbate affinity and that the adsorption at one site does not affect the adsorption at an adjacent site. The results confirmed the formation of a monolayer of mercury ions on the surface of Fe_3O_4-GNS-NH_2 hybrids. In addition, the adsorption capacity (Q_{max}) of Fe_3O_4-GNS-NH_2 hybrids for Hg(II) was obtained as 96.15 mg/g which was higher than some Q_{max} values of other sorbents reported by literatures (Table 3).

A further analysis of the Langmuir equation, the essential feature of the Langmuir adsorption can be expressed by means of R_L [37]. R_L is a dimensionless equilibrium parameter for predicting whether an adsorption system is favorable or unfavorable which is given by:

$$R_L = \frac{1}{1 + K_L C_0} \quad (4)$$

where C_0 is the initial Hg(II) concentration ($mg\,L^{-1}$) and K_L is Langmuir constant ($L\,mg^{-1}$). The value of R_L reveals the nature of the adsorption process: the value of R_L lies between 0 and 1 for a favorable adsorption, $R_L > 1$ represents an unfavorable adsorption, $R_L = 1$ shows the linear adsorption, and the adsorption operation is irreversible if $R_L = 0$.

In our study, the calculated R_L values for the adsorption on the Fe_3O_4-GNS-NH_2 hybrids at initial concentration range from 5 to 300 $mg\,L^{-1}$. According to the value of K_L listed in Table 2, the R_L values obtained are between 0 and 1, indicating the adsorption is favorable.

3.2.6. Adsorption kinetics of Hg(II)

The pseudo- first order adsorption and the pseudo-second-order adsorption [38–41] were used to fit kinetics experimental data, in order to investigate the controlling mechanism involved in the removal of heavy metals, such as mass transport and the chemical reaction process. The above two kinetics equations are described as:

$$\log(Q_e - Q_t) = \log Q_e - \frac{k_1 t}{2.303} \quad (5)$$

Table 2
The Langmuir and Freundlich equations, the values of parameters and correlation coefficients (20℃, pH 6)

Models	Constants		R	Equations
Langmuir	$Q_{\max}$ (mg/g)	96.15	0.9992	$\frac{C_e}{Q_e} = 0.0145 + 0.0104C_e$
	K_L (L/mg)	0.7172		
Freundlich	$K_F \times 10^{-3}$ ((L/mg)$^{1/n}$)	4.3627	0.8573	$\text{In}Q_e = 1.4731 + 0.4282\,\text{In}C_e$
	n (mg/L)	2.335		

Table 3
Comparison of Hg(II) adsorption capacity of Fe_3O_4-GNS-NH_2 with other sorbents

Sorbent	$Q_{\max}$ (mg /g)	Temperature (℃)	Initial pH	References
PS	1.90	25	3.0	[17]
MPS	30.72	25	3.0	[17]
Activated carbon	60	25	6.0	[15]
Magnetically modified yeast cells	93	25	6.0	[16]
Fe_3O_4-GNS-NH_2	96.15	20	6.0	Present work

Table 4
The adsorption kinetic model rate constants for Hg(II) on Fe_3O_4-GNS-NH_2 hybrids at initial Hg(II) concentrations of 100 mg/L (20℃, pH 6)

Models	Initial concentration	Constants		R	Equations
Pseudo- first order	100 mg/L	k_1 (L/min)	0.072	0.8503	$\log(Q_e - Q_t) = 0.9441 - 0.0311t$
		Q_e (Cal) (mg/g)	8.79		
Pseudo- second order	100 mg/L	k_2 (g/mg min)	1.324	0.9992	$\frac{t}{Q_t} = 0.0200t + 0.05$
		Q_e (Cal) (mg/g)	50.00		

$$\frac{t}{Q_t} = \frac{1}{K_2 Q_e^2} + \frac{t}{Q_{e2}} \tag{6}$$

where Q_t and Q_e are the adsorption capacity (mg g^{-1}) at various time t and equilibrium time, k_1 and k_2 are the pseudo-first-order rate constant (min^{-1}) and pseudo-second-order rate constant (g mg^{-1} min^{-1}).

The calculated parameters and correlation coefficients (R) of the above described kinetics equations are given in Table 4. From Table 4, it can be seen that the adsorption data is well fitted by pseudo-second-order kinetic with a much higher correlation coefficient (0.9912) than the pseudo-first-order kinetic. The results suggested that metal ions sorption by Fe_3O_4-GNS-NH_2 hybrids can be explained by the pseudo-second-order mechanism which further revealed that the process controlling the rate was a chemical sorption. The results are consistent with the XPS analysis, which the main adsorption mechanism of metal ions sorption by Fe_3O_4-GNS-NH_2 hybrids was the formation of N-metal ions chemical complex.

4. Conclusions

(1) Amino-functionalized graphite nanosheets decorated with Fe_3O_4 nanoparticles were successfully used as adsorbent for the removal of Hg(II) from aqueous solution with pH range from 4.0 to 6.0.

(2) The results of XPS analyses indicated that Hg (II) was completely reduced to Hg(I) via electron transport from amino sites of the Fe_3O_4-GNS-NH_2 to mercury, which was the formation of N-metal ions chemical complex in the adsorption process.

(3) The Langmuir isotherm model was found to be suitable for the Hg(II) adsorption and the adsorption kinetic followed the pseudo-second-order equation for Fe_3O_4-GNS-NH_2 hybrids, which revealed that the adsorption process was a chemical sorption by the formation of a monolayer of mercury ions on the surface of Fe_3O_4-GNS-NH_2 hybrids.

Acknowledgements

The work was financially supported by the National Natural Science Foundation of China (grant number 51403091), the Natural Science Foundation of Gansu Province (grant number 2013GS09508) and the Opening Foundation of State Key Laboratory of Advanced Processing and Recycling of Non-ferrous Metals of China (grant number SKL1315).

References

[1] H. Tang, C.Y. Chang, L.N. Zhang, Efficient adsorption of Hg^{2+} ions on chitin/cellulose composite membranes prepared via environmentally friendly pathway, Chem. Eng. J. 173 (2011) 689–697.

[2] M. De, R. Azargohar, A.K. Dalai, S.R. Shewchuk, Mercury removal by bio-char based modified activated carbons, Fuel 103 (2013) 570–578.

[3] M.J. Shadbad, A. Mohebbi, A. Soltani, Mercury(II) removal from aqueous solutions by adsorption on multi-walled carbon nanotubes, J. Chem. Eng. 28(4) (2011) 1029–1034.

[4] D. Zhou, L. Zhang, S. Guo, Mechanisms of lead biosorption on cellulose/chitin beads, Water Res. 39 (2005) 3755–3762.

[5] S. Haider, S. Park, Preparation of the electrospun chitosan nanofibers and their applications to the adsorption of Cu(II) and Pb(II) ions from an aqueous solution, J. Membr. Sci. 328 (2009) 90–96.

[6] U. Gunten, Ozonation of drinking water. Part I. Oxidation kinetics and product formation, Water Res. 37 (2003) 1443–1467.

[7] G. Steenkamp, K. Keizer, H. Neomagus, H. Krieg, Copper(II) removal from polluted water with alumina/chitosan composite membranes, J. Membr. Sci. 197 (2002) 147–156.

[8] Z. Reddad, C. Gerente, Y. Andres, J. Thibault, P. Cloirec, Cadmium and lead adsorption by a natural polysaccharide in MF membrane reactor: Experimental analysis and modelling, Water Res. 37 (2003) 3983–3991.

[9] M. Beppu, E. Arruda, R. Vieira, N. Santos, Adsorption of Cu(II) on porous chitosan membranes functionalized with histidine, J. Membr. Sci. 240 (2004) 227–235.

[10] S. Kobayashi, A. Makino, H. Matsumoto, S. Kunii, M. Ohmae, T. Kiyosada, K. Makiguchi, A. Matsumoto, M. Horie, S.I. Shoda, Enzymatic polymerization to novel polysaccharides having a glucose-N-acetylglucosamine repeating unit, a cellulose−chitin hybrid polysaccharide, Biomacromolecules 7 (2006) 1644–1656.

[11] S.D. Pan, Y. Zhang, H.Y. Shen, M.Q. Hu, An intensive study on the magnetic effect of mercapto-functionalized nano-magnetic Fe_3O_4 polymers and their adsorption mechanism for the removal of Hg(II) from aqueous solution, Chem. Eng. J. 210 (2012) 564–574.

[12] K. Mandel, F. Hutter, C. Gellermann, G. Sextl, Modified superparamagnetic nanocomposite microparticles for highly selective Hg(II) or Cu(II) separation and recovery from aqueous solutions, Appl. Mater. Interfaces 4(10) (2012) 5633–5642.

[13] S.D. Pan, H.Y. Shen, Q.H. XuJ. Luo M.Q. Hu, Surface mercapto engineered magnetic Fe_3O_4 nanoadsorbent for the removal of mercury from aqueous solutions, J. Colloid Interface Sci. 365(1) (2012) 204–212.

[14] E.K. Faulconer, N.V. Von Reitzenstein, D.W. Mazyck, Optimization of magnetic powdered activated carbon for aqueous Hg(II) removal and magnetic recovery, J. Hazard. Mater. 199–200 (2012) 9–14.

[15] J.Z. Zhu, B.L. Deng, J. Yang, D.C. Gang, Modifying activated carbon with hybrid ligands for enhancing aqueous mercury removal, Carbon 47 (2009) 2014–2025.

[16] H. Yavuz, A. Denizli, M. Safarikova, I. Safarik, Biosorption of mercury on magnetically modified yeast cells, Sep. Purif. Technol. 52 (2006) 253–260.

[17] Y. Liu, X.M. Sun, B.H. Li, Adsorption of Hg^{2+} and Cd^{2+} by ethylenediamine modified peanut shells, Carbohydr. Polym. 81 (2010) 335–339.

[18] Z. Liu, H.S. Wang, C. Liu, Y.J. Jiang, G. Yu, X.D. Mu, X.Y. Wang, Magnetic cellulose–chitosan hydrogels prepared from ionic liquids as reusable adsorbent for removal of heavy metal ions, Chem. Commun. 48(59) (2012) 7350–7352.

[19] M. Monier, D.A. Abdel-Latif, Preparation of cross-linked magnetic chitosan-phenylthiourea resin for adsorption of Hg(II), Cd(II) and Zn(II) ions from aqueous solutions, J. Hazard. Mater. 209–210 (2012) 240–249.

[20] R. Sengupta, M. Bhattacharya, S. Bandyopadhyay, A.K. Bhowmick, A review on the mechanical and electrical properties of graphite and modified graphite reinforced polymer composites, Prog. Polym. Sci. 36 (2011) 638–670.

[21] H.L. Guo, X.F. Wang, Q.Y. Qian, F.B. Wang, X.H. Xia, A green approach to the synthesis of graphene nanosheets, ACS Nano. 3 (2009) 2653–2659.

[22] G. Zhao, X. Ren, X. Gao, X. Tan, J. Li, C. Chen, Y. Huang, X. Wang, Removal of Pb(II) ions from aqueous solutions on few-layered graphene oxide nanosheets, Dalton Trans. 40 (2011) 10945–10952.

[23] S.L. Luo, X.L. Xu, G.Y. Zhou, C.B. Liu, Y.H. Yang, Y.T. Liu, Amino siloxane oligomer-linked graphene oxide as an efficient adsorbent for removal of Pb(II) from wastewater, J. Hazard. Mater. 274 (2014) 145–155.

[24] F. Fang, L.T. Kong, J.R. Huang, S.B. Wu, K.S. Zhang, X.L. Wang, B. Sun, Z. Jin, J. Wang, X.J. Huang, J.H. Liu, Removal of cobalt ions from aqueous solution by an amination graphene oxide nanocomposite, J. Hazard. Mater. 270 (2014) 1–10.

[25] Y.X. Ma, Y.F. Li, G.H. Zhao, L.Q. Yang, J.Z. Wang, X. Shan, X. Yan, Preparation and characterization of graphite nanosheets decorated with Fe_3O_4 nanoparticles used in the immobilization of glucoamylase, Carbon 50(8) (2012) 2976–2986.

[26] T.V. Ramakrishna, G. Aravamudan, M. Viyajakumar, Spectrophotometric determination of mercury(II) as the ternary complex with rhodamine 6g and iodide, Anal. Chim. Acta 84(2) (1976) 369–375.

[27] R.S. Vieira, M.L.M. Oliveira, E. Guibal, E. Rodríguez-Castellón, M.M. Beppu, Copper, mercury and chromium adsorption on natural and crosslinked chitosan films: An XPS investigation of mechanism, Colloids Surf., A 374 (2011) 108–114.

[28] X.L. Li, Z.F. Ye, Y. Zhang, X.J. Ma, L.Q. Yang, Y.F. Li, Efficient removal of Hg(II) by polymer-supported hydrated metal oxides from aqueous solution, Sep. Sci. Technol. 47 (2012) 729–741.

[29] A.I. Zouboulis, K.A. Kydros, K.A. Matis, Removal of hexavalent chromium anions from solutions by pyrite fines, Water Res. 29 (1995) 1755–1760.

[30] X.J. Ma, Y.F. Li, Z.F. Ye, L.Q. Yang, L.C. Zhou, L.Y. Wang, Novel chelating resin with cyanoguanidine group: Useful recyclable materials for Hg(II) removal in aqueous environment, J. Hazard. Mater. 185 (2011) 1348–1354.

[31] W.R. Knocke, L.H. Hemphill, Mercury(II) sorption by waste rubber, Water Res. 15 (1981) 275–282.

[32] A. Walcabius, J. Devoy, J. Bessiere, Electrochemical recognition of selective mercury adsorption on minerals, Environ. Sci. Technol. 33 (1999) 4278–4284.

[33] S.K. Das, A.R. Das, A.K. Guha, A study on the adsorption mechanism of mercury on aspergillus versicolor biomass, Environ. Sci. Technol. 41 (2007) 8281–8287.

[34] I. Langmuir, The adsorption of gases on plane surfaces of glass, mica and platinum, J. Am. Chem. Soc. 40 (1918) 1361–1403.

[35] H. Freundlich, W. Heller, The adsorption of cis- and trans-azobenzene, J. Am. Chem. Soc. 61 (1939) 2228–2230.

[36] O. Altin, H.O. Ozbelge, T. Dogu, Use of general purpose adsorption isotherms for heavy metal–clay mineral interactions, J. Colloid Interface Sci. 198 (1998) 130–140.

[37] M. Ahmaruzzaman, D.K. Sharma, Adsorption of phenols from wastewater, J. Colloid Interface Sci. 287 (2005) 14–24.

[38] V. Srihari, A. Das, The kinetic and thermodynamic studies of phenol-sorption onto three agro-based carbons, Desalination 225 (2008) 220–234.

[39] Y. Zhang, X.L. Li, W. Zheng, Z.F. Ye, Y.F. Li, Enhanced removal of Pb^{2+} from water by adsorption onto phosphoric acid-modified PS-EDTA resin: Mechanism and kinetic study, Desalin. Water Treat. 51 (2013) 7223–7235.

[40] G. Crini, H.N. Peindy, F. Gimbert, C. Robert, Removal of C.I. basic green 4 (malachite green) from aqueous solutions by adsorption using cyclodextrin-based adsorbent: Kinetic and equilibrium studies, Sep. Purif. Technol. 53 (2007) 97–110.

[41] L.Q. Yang, Y.F. Li, L.Y. Wang, Y. Zhang, X.J. Ma, Z.F. Ye, Preparation and adsorption performance of a novel bipolar PS-EDTA resin in aqueous phase, J. Hazard. Mater. 180 (2010) 98–105.